Journal of Magnetic Resonance **146,** 33–42 (2000)
doi:10.1006/jmre.2000.2111, available online at http://www.idealibrary.com on IDEAL®

Simulations of Chemical Exchange Lineshapes in CP/MAS Spectra Using Floquet Theory and Sparse Matrix Methods

P. Hazendonk, Alex D. Bain,[1] H. Grondey,* P. H. M. Harrison, and R. S. Dumont

Department of Chemistry, McMaster University, 1280 Main St. W, Hamilton, Ontario L8S 4M1, Canada; and
**Department of Chemistry, University of Toronto, Toronto, Ontario M5S 3H6, Canada*

Received October 11, 1999; revised April 28, 2000

This paper presents a general method for simulating the effect of chemical exchange on MAS NMR spectra of solid samples. The complication in MAS spectra is that the Hamiltonian itself is time-dependent, due to the spinning of the sample. The approach taken in this work is to use Floquet theory to convert the problem into a time-independent form, and then use established methods (used in liquid NMR simulations) to calculate the lineshape. Floquet theory has been admired for its elegance, but criticized for its computational inefficiencies. This is because it removes the time dependence of the system by expanding the problem in a Fourier-like series. This makes a relatively small, time-dependent calculation into a much larger time-independent one. Typically, we use twice as many Floquet blocks as there are spinning sidebands, so the increase in size is substantial. The problem that this creates stems from the fact that the usual Householder methods for diagonalizing a matrix scale as the cube of the size of the matrix. This would make a Floquet calculation prohibitively long. However, the Floquet matrix is inherently sparse, so sparse matrix methods can produce substantial computational savings. Also, fully diagonalizing a matrix is expensive, but converting the matrix to a tridiagonal form (using iterative Lanczos methods) is much cheaper. The use of the Lanczos methods makes the Floquet calculations feasible as a general method for systems of more than one spin. We show how to set up the full matrix describing chemical exchange in a spinning sample, but the details of how the Lanczos methods work are not included—they are described elsewhere. We then validate the theory by simulating the MAS spectra of dimethyl sulfone both with natural abundance ^{13}C and with methyl groups labeled with ^{13}C. The latter system has both dipolar and chemical shielding anisotropy terms contributing to the spectrum.

Key Words: **chemical exchange; CP/MAS; Floquet theory; spinning sidebands.**

INTRODUCTION

The use of cross-polarization (CP) and magic-angle spinning (MAS) in obtaining the NMR spectra of solid samples is well known (*1*). The lineshape changes in the NMR spectra of liquid samples, due to chemical exchange, are also very familiar (*2, 3*). However, there are relatively few rigorous studies of the effects of chemical exchange on the patterns of spinning sidebands observed in CP/MAS spectra of complex spin systems. This is because the Hamiltonian is time-dependent, and the spectrum is relatively complicated to calculate (compared to liquids). For simple solid systems (*4*), exchange effects are often treated in the same way as liquid spectra, using the standard Kubo and Tomita (*5*) or Gutowsky and Holm formalism (*6*). To provide a full and general description, it is necessary to combine the rigorous treatment of liquids with the complexities of the MAS experiment.

In this work we use Floquet theory (*7–17*) to convert the time-dependent MAS problem into a time-independent (but much larger) description. This is not a new approach (*18*), but it has been hampered by the size of the matrices generated. However, the Floquet matrices are inherently sparse. As such, modern sparse matrix methods reduce the numerical difficulties dramatically. We use the dual Lanczos method (*19–24*) in Wassam's formulation (*25, 26*) to tridiagonalize the resulting matrices. For large matrices, this is much more efficient than the usual Householder method (*27*). The general formalism is developed and applied to the simulation of the MAS ^{13}C NMR spectra of doubly ^{13}C-labeled dimethyl sulfone.

Floquet theory was introduced to spectroscopic problems by Shirley (*28*), who applied this theory to compute the propagator corresponding to a time-dependent non-self-commuting Hamiltonian. This is achieved by changing to a Fourier-spin space, where the Hamiltonian is time-independent, but infinite in dimension. Using similar methods, Vega described multiple-quantum effects in double-frequency pulsed NMR experiments on spin-1/2 and 1 systems (*29–31*). Later Zax and Vega used Floquet methods to design broadband pulses (*32, 33*). Vega also applied Floquet theory to compute sideband patterns of rotating solids. This led to expressions for sideband intensities that were similar to those by Herzfeld and Berger (*34*) and Maricq and Waugh (*35*). For multispin systems, numerical methods are required. Based on a perturbation method proposed by Maricq (*36*), spectra of coupled spin pairs were computed to model rotational resonance (*13–15, 17, 37*) and REDOR dephasing curves (*12, 38*). Schmidt and Vega applied Floquet theory to uncoupled exchange in rotating solids using the Bloch–McConnell approach (*18, 39, 40*). In this case, only

[1] To whom correspondence should be addressed.

1090-7807/00 $35.00

numerical diagonalization was possible for the general solution. However, in both the slow and the fast exchange regimes it was possible to derive eigenvalues and diagonalization matrices using perturbation theory along with the solutions to the static one-spin case (*18*).

General principles of Floquet theory, as applied to NMR, have been discussed in several papers (*7–17*). The Hamiltonian (or in our case, the Liouvillian) has a periodic time dependence, due to the magic-angle spinning. The Floquet approach expands the evolving spin state into something resembling Fourier components at multiples of the spinning speed. The time evolution of this collection of component spin states, treated as a single vector, is governed by a *time-independent* effective Hamiltonian (or Liouvillian). In principle, there is an infinite number of components, but in practice the number is often truncated to roughly twice the number of spinning sidebands with significant intensity. This turns a relatively small, time-dependent problem into a time-independent problem which has matrices that may be 30 to 40 times larger.

CHEMICAL EXCHANGE

Chemical exchange affects the NMR spectrum, since the magnetic environment of a nucleus is changed by the exchange (*2, 3*). A single transition in one site will have its frequency changed, and may even be split among several transitions in the other site. Because exchange involves an evolution of the site populations and coherences, which are combinations of density matrix elements, a density matrix description is needed. The density matrix is conveniently treated in Liouville space, a vector space in which the density matrix appears as a vector (*41–43*). This vector can be regarded as a list of all possible observables of the system. Its time evolution is governed by the Liouville–von Neumann equation,

$$\frac{\partial}{\partial \mathrm{t}}\rho = -\mathrm{i}\mathbf{L}\rho, \qquad [1]$$

where $\mathbf{L}$ is the Liouville superoperator (or Liouvillian), obtained from the commutator with the Hamiltonian (*44, 45*). Superoperators are represented as simple matrices in Liouville space.

The effects of chemical exchange and relaxation are also represented as matrices, which add a dissipative term to the time evolution of the density matrix. The Redfield matrix is the description of relaxation, and exchange is described by a Kubo–Sack-type matrix. Exchange couples the sites, so for a two-site exchange, the equation of motion of the two density matrices will have the form

$$\frac{\partial}{\partial \mathrm{t}}\begin{pmatrix}\rho_1\\ \rho_2\end{pmatrix} = \begin{pmatrix}-\mathrm{i}\mathbf{L}_1 - \mathbf{K}_{12} & \mathbf{K}_{21}\\ \mathbf{K}_{12} & -\mathrm{i}\mathbf{L}_2 - \mathbf{K}_{21}\end{pmatrix}\begin{pmatrix}\rho_1\\ \rho_2\end{pmatrix}. \qquad [2]$$

In this equation, it is clear that in the absence of exchange, the two sites will evolve independently under the Liouvillians $\mathbf{L}_1$ and $\mathbf{L}_2$. The chemical exchange terms ($\mathbf{K}_{12}$ represents coherence leaving site 1 for site 2) couple the two sites together. We can combine the Liouvillians and the exchange matrices into one big matrix, and we can write Eq. [2] in the composite space of all the exchanging sites as in

$$\frac{\partial}{\partial \mathrm{t}}\rho = (-\mathrm{i}\mathbf{L} - \mathbf{K})\rho. \qquad [3]$$

The time-domain solution to Eq. [3] can be written as in the following equation, since it is a first-order set of equations:

$$\rho(\mathrm{t}) = \exp[(-\mathrm{i}\mathbf{L} - \mathbf{K})\mathrm{t}]\rho(0). \qquad [4]$$

Taking the Fourier transform of [4] gives us the frequency-domain solution, as in

$$\rho(\nu) = (2\pi\mathrm{i}\nu\mathbf{1} - \mathrm{i}\mathbf{L} - \mathbf{K})^{-1}\rho_{\mathrm{eq}}, \qquad [5]$$

in which $\mathbf{1}$ represents the unit matrix, ν represents frequency, and ρ_{eq} is the result of applying a hard $\pi/2$ pulse to the equilibrium density matrix.

These equations give the density matrix as a function of either time or frequency. The observable spectrum is just the trace of the density matrix with the total $\mathbf{I}_x$ spin operator, since it is the total x magnetization that is observed. This trace becomes a simple dot product in Liouville space, so the spectrum is given by

$$\begin{aligned}\text{spectrum} &= \mathbf{I}_x \cdot \rho(\nu)\\ &= \mathbf{I}_x \cdot (2\pi\mathrm{i}\nu\mathbf{1} - \mathrm{i}\mathbf{L} - \mathbf{K})^{-1}\rho_{\mathrm{eq}}.\end{aligned} \qquad [6]$$

There are several ways to use these equations to calculate a spectrum. In the time domain, we could calculate an FID using [4] and then Fourier transform the FID to obtain a spectrum. In the frequency domain, we could perform the matrix inversion in [6] for each value of ν and trace the spectrum point by point. The standard way of doing this calculation, however, is to first diagonalize the matrix $(-\mathrm{i}\mathbf{L} - \mathbf{K})$. In this representation, the matrix inversion in [6] (as a function of ν) is trivial, and the diagonalization need only be done once (*46*).

For large systems, this standard solution is not feasible. The computational effort to diagonalize a matrix, using Householder methods, scales as the cube of the size of the matrix (*27*). For a system of spin-1/2 nuclei, this means that adding a spin increases the calculation time by roughly a factor of 64 (since the size of the Liouville space goes up by a factor of 4). In the time domain, this problem can be avoided by explicitly propagating the superoperator $-\mathrm{i}\mathbf{L} - \mathbf{K}$ using Chebyshev evolution and sparse matrix representations (*47*). There are considerable overheads in this calculation, but for larger spin

systems, the direct evolution is much more efficient. Chebyshev evolution is an excellent method (*48*) when there is no dissipation. The effects of chemical exchange are then incorporated via a split-operator method, in which the evolution and exchange are alternately propagated for short periods. This approach is useful when the experiment involves some time evolution, as in a pulse sequence, but it is not necessary for the calculation of the simple spectrum (*24*). The Lanczos methods are better for simple spectrum calculation.

In the frequency-domain method, converting $-i\mathbf{L} - \mathbf{K}$ to a diagonal matrix is generally expensive, but converting it to a tridiagonal form can be much cheaper. The linear equations derived from the tridiagonal matrix can then be solved by the relatively efficient LU decomposition (*19*). The dual Lanczos method (*19*) is an iterative technique for tridiagonalization which scales much more gently (*24*) than the cube of the size of the matrix (between first and second orders). Lanczos methods are based on repeated applications of the matrix to some starting vector, which can be done very efficiently for sparse matrices. These repeated applications generate a series of vectors, which span a space called the Krylov subspace (*19*). The Lanczos algorithm makes these vectors orthonormal in a numerically stable way, and eventually produces a basis for the whole space, called the Lanczos representation. In this representation, the tridiagonal form of $-i\mathbf{L} - \mathbf{K}$ is used in Eq. [6]. This equation can be solved for each frequency and the spectrum can be traced out. There are considerable overheads, but for large systems, the scaling with respect to matrix size can approach linear. Details of the implementation of Lanczos methods to chemical exchange are described elsewhere (*24*).

The Lanczos method is based on a recursion formula, which generates a set of vectors, describing the Lanczos representation, and a tridiagonal form of the matrix in question. Each iteration involves a sparse matrix–vector multiply, which scales with the order of the matrix, O. Therefore, the Lanczos tridiagonalization process scales as $O \times N_L$, where N_L is the number of iterations required for convergence. The direct spectrum computation described above requires $N_L \times N_\nu$ operations, where N_ν is the number of frequency points in the spectrum. This is the result of the LU decomposition scaling linearly with the matrix order for a tridiagonal system. For small systems the spectrum calculation is expected to dominate the computation time since N_ν is much larger than O, and N_L is approximately equal to O. For large systems, the spectrum is crowded and N_L can be much smaller than O, which is an effect called saturation. In this case, the scaling will be approximately linear. For intermediate sized systems the scaling will be O^2 since N_L is approximately equal to O.

CHEMICAL EXCHANGE IN CP/MAS SPECTRA

In order to apply the approach of the previous section, we must convert the time-dependent Liouvillian for the spinning sample into something that is time-independent. We start this process by looking at the time dependence of the Hamiltonian in the frame of reference of the rotor. A spin Hamiltonian is just the sum of 3×3 quadratic forms, such as $\mathbf{B}^T\boldsymbol{\sigma}\mathbf{I}$ or $\mathbf{I}^T\mathbf{D}\mathbf{S}$, where $\mathbf{B}$ is the magnetic field, $\mathbf{I}$ and $\mathbf{S}$ are spin operators, $\boldsymbol{\sigma}$ is the chemical shielding tensor, and $\mathbf{D}$ is the dipolar tensor. The spin operators are the usual I_x, I_y, and I_z operators. If α is the angle of rotation about the z axis, then the effect of this rotation on the spin operators is given by $\mathbf{R}(\alpha)\mathbf{I}$, where $\mathbf{R}$ is given in

$$\begin{aligned}\mathbf{R}(\alpha) &= \begin{pmatrix} \cos\alpha & -\sin\alpha & 0 \\ \sin\alpha & \cos\alpha & 0 \\ 0 & 0 & 1 \end{pmatrix} \\ &= \begin{pmatrix} 0 & 0 & 0 \\ 0 & 0 & 0 \\ 0 & 0 & 1 \end{pmatrix} + e^{i\alpha}\begin{pmatrix} 1/2 & i/2 & 0 \\ -i/2 & 1/2 & 0 \\ 0 & 0 & 0 \end{pmatrix} \\ &\quad + e^{-i\alpha}\begin{pmatrix} 1/2 & -i/2 & 0 \\ i/2 & 1/2 & 0 \\ 0 & 0 & 0 \end{pmatrix}. \end{aligned} \quad [7]$$

If $\mathbf{M}$ is a tensor in this frame, then the effect of the rotation is given by

$$\mathbf{M}(\alpha) = \mathbf{R}(\alpha)\mathbf{M}(0)\mathbf{R}^T(\alpha). \quad [8]$$

If we substitute [7] into [8], we get a five-term Fourier series for $\mathbf{M}(\alpha)$, given in

$$\mathbf{M}(\alpha) = \sum_{j=-2}^{2} \mathbf{M}^{(j)} e^{ij\alpha}, \quad [9]$$

where the superscript j denotes the Fourier component. These Fourier components can be written explicitly in terms of the matrix elements of $\mathbf{M}$,

$$\mathbf{M}^{(0)} = \begin{pmatrix} \dfrac{(M_{11} + M_{22})}{2} & 0 & 0 \\ 0 & \dfrac{(M_{11} + M_{22})}{2} & 0 \\ 0 & 0 & M_{33} \end{pmatrix} \quad [10]$$

$$\mathbf{M}^{(\pm 1)} = \begin{pmatrix} 0 & 0 & \dfrac{(M_{31} \pm iM_{32})}{2} \\ 0 & 0 & \dfrac{(M_{32} \mp iM_{31})}{2} \\ \dfrac{(M_{31} \pm iM_{32})}{2} & \dfrac{(M_{32} \mp iM_{31})}{2} & 0 \end{pmatrix} \quad [11]$$

$$\mathbf{M}^{(\pm 2)} = \begin{pmatrix} \dfrac{(M_{11} - M_{22} \pm 2iM_{12})}{4} \\ \dfrac{(\mp iM_{11} \pm iM_{22} + 2M_{12})}{4} \\ 0 \end{pmatrix} \times \begin{pmatrix} \dfrac{(\mp iM_{11} \pm iM_{22} + 2M_{12})}{4} & 0 \\ \dfrac{(-M_{11} + M_{22} \mp 2iM_{12})}{4} & 0 \\ 0 & 0 \end{pmatrix}. \quad [12]$$

Note that the symmetry of **M** has been used in these equations. Equation [9] gives us the Fourier expansion of the Hamiltonian—the fact that there are five terms arises from the second-rank nature of the tensors. From the Hamiltonian, we can calculate the propagators of the density matrix.

In Floquet theory, the propagator is also expanded into something resembling a Fourier series. The series is infinite, but it can be truncated to leave a much larger, but still finite, propagator. Because of the five terms in [9], the matrix representation of the propagator has a pentadiagonal structure—the other off-diagonal terms are zero. The Floquet representation produces, therefore, a large, sparse matrix.

In order to calculate the propagator for a system with chemical exchange, we work exclusively with the Liouvillian, the commutator with the Hamiltonian. Because the Hamiltonian has a five-term Fourier expansion in terms of rotation about the rotor axis, so will the Liouvillian, $\mathbf{L}(t)$. This is expressed in

$$\mathbf{L}(t) = \sum_{j=-2}^{2} \mathbf{L}^{(j)} e^{ij\omega t}, \quad [13]$$

where the angle of rotation is the product of the spinning speed, ω, and time, t.

The density matrix, as a function of time, is given by some unknown propagator **U**, as in

$$\rho(t) = \mathbf{U}(t)\rho(0). \quad [14]$$

The propagator is more complicated than in Eq. [4], since **L** is itself time-dependent. However, we can expand the propagator in a series as

$$\mathbf{U}(t) = \sum_{k=-\infty}^{\infty} \mathbf{U}^{(k)}(t) e^{ik\omega t}. \quad [15]$$

Note that this is not a Fourier series, since the components still carry some time dependence. We must now solve for that dependence.

Since $\rho(t)$ satisfies the Liouville–von Neumann equation, the propagator, **U**, must satisfy the matrix equation

$$\frac{\partial}{\partial t}\mathbf{U}(t) = -i\mathbf{L}(t)\mathbf{U}(t). \quad [16]$$

If we substitute [13] and [15] into [16], we get

$$\sum_{k=-\infty}^{\infty} \frac{\partial}{\partial t}(\mathbf{U}^{(k)}(t)e^{ik\omega t}) = -i \sum_{j=-2}^{2} \sum_{k=-\infty}^{\infty} \mathbf{L}^{(j)}\mathbf{U}^{(k)}(t)e^{i(j+k)\omega t}. \quad [17]$$

Taking the derivative of the product on the left, and rearranging, gives the following equation, in which δ_{j0} is the Kronecker delta and **1** is the unit matrix:

$$\sum_{k=-\infty}^{\infty} \left(\frac{\partial}{\partial t}\mathbf{U}^{(k)}(t)\right) e^{ik\omega t} = -i \sum_{k=-\infty}^{\infty} \sum_{j=-2}^{2} (\mathbf{L}^{(j)} + k\omega\delta_{j0}\mathbf{1})\mathbf{U}^{(k)}(t)e^{i(k+j)\omega t}. \quad [18]$$

The k index on the left is arbitrary, so Eq. [18] can be rewritten as

$$\sum_{k=-\infty}^{\infty} \left(\frac{\partial}{\partial t}\mathbf{U}^{(k)}(t)\right) e^{ik\omega t} = -i \sum_{k=-\infty}^{\infty} \sum_{j=-2}^{2} (\mathbf{L}^{(j)} + (k-j)\omega\delta_{j0}\mathbf{1})\mathbf{U}^{(k-j)}(t)e^{ik\omega t}. \quad [19]$$

The solution to this equation is unique, so it is satisfied by the solutions of the following equation, for all values of k:

$$\frac{\partial}{\partial t}\mathbf{U}^{(k)}(t) = -i \sum_{j=-2}^{2} (\mathbf{L}^{(j)} + (k-j)\omega\delta_{j0}\mathbf{1})\mathbf{U}^{(k-j)}(t). \quad [20]$$

If we solve these equations for the Floquet components of the propagator, they can be substituted into [15] and [14], to give the density matrix as a function of time (*40*).

Let us write all the propagators, $\mathbf{U}^{(k)}$ as an infinite vector, $\mathbf{U}$, as in

$$\mathbf{U}(t) = \begin{pmatrix} \vdots \\ \mathbf{U}^{(+2)} \\ \mathbf{U}^{(+1)} \\ \mathbf{U}^{(0)} \\ \mathbf{U}^{(-1)} \\ \mathbf{U}^{(-2)} \\ \vdots \end{pmatrix}. \qquad [21]$$

Equation [20] can then be written as

$$\frac{\partial}{\partial t}\mathbf{U}(t) = -i\mathbf{L}\mathbf{U}(t), \qquad [22]$$

where $\mathbf{L}$ is given by

$$\mathbf{L} = \begin{pmatrix} \ddots & \ddots & \ddots & \ddots \\ \ddots & \mathbf{L}^{(0)} + 2\omega & \mathbf{L}^{(+1)} & \mathbf{L}^{(+2)} \\ \ddots & \mathbf{L}^{(-1)} & \mathbf{L}^{(0)} + \omega & \mathbf{L}^{(+1)} \\ \ddots & \mathbf{L}^{(-2)} & \mathbf{L}^{(-1)} & \mathbf{L}^{(0)} \\ \ddots & 0 & \mathbf{L}^{(-2)} & \mathbf{L}^{(-1)} \\ \ddots & 0 & 0 & \mathbf{L}^{(-2)} \\ \ddots & \ddots & \ddots & \ddots \end{pmatrix} \times \begin{pmatrix} \ddots & \ddots & \ddots \\ 0 & 0 & \ddots \\ \mathbf{L}^{(+2)} & 0 & \ddots \\ \mathbf{L}^{(+1)} & \mathbf{L}^{(+2)} & \ddots \\ \mathbf{L}^{(0)} - \omega & \mathbf{L}^{(+1)} & \ddots \\ \mathbf{L}^{(-1)} & \mathbf{L}^{(0)} - 2\omega & \ddots \\ \ddots & \ddots & \ddots \end{pmatrix}. \qquad [23]$$

This is a general equation. If we are including the effects of chemical exchange, then each of the $\mathbf{L}$ terms is composite, made up from the individual sites, as in Eq. [2] and Eq. [3]. The off-diagonal elements $\mathbf{L}^{(+/-1)}$ and $\mathbf{L}^{(+/-2)}$ are equal to the composite of $\mathbf{L}^{(+/-1)}$ and $\mathbf{L}^{(+/-2)}$ in Eq. [13]. It is important to note that the time dependence of these matrix elements comes from the mechanical rotation, which affects the spatial parts of the interaction. However, since the exchange matrix, $\mathbf{K}$, is time-independent it contributes only to $\mathbf{L}^{(0)}$. Chemical exchange thus only affects the diagonal elements of $\mathbf{L}$, which have the form of Eq. [2]. We can therefore construct the whole matrix, $\mathbf{L}$, from the Liouvillians of the individual sites and the exchange matrix, $\mathbf{K}$.

We solve Eq. [22] in the same way as any set of first-order differential equations, to give

$$\mathbf{U}(t) = \exp(-i\mathbf{L}t)\mathbf{U}(0). \qquad [24]$$

Note that at t = 0, no propagation has occurred. This means that in Eq. [21], $\mathbf{U}^{(0)}(t)$ is the unit operator, and all other $\mathbf{U}^{(j)}(t)$ are zero at t = 0. If we divide $\exp(-i\mathbf{L}t)$ into blocks, as in Eq. [23], then any individual propagator, $\mathbf{U}^{(j)}(t)$, at time t is the (j, 0) block of $\exp(-i\mathbf{L}t)$, as given by

$$\mathbf{U}^{(j)}(t) = [\exp(-i\mathbf{L}t)]_{j,0}. \qquad [25]$$

We now have the description of the density matrix evolution. The elements of the matrix, $\mathbf{L}$, are constructed from the individual site Liouvillians, with the exchange rate contributing only to the diagonal elements. These are then assembled into the form of Eq. [23], and the exponential is calculated. From this exponential, we can extract each propagator, as in [25]. If we substitute these into [14] and [15], we get

$$\rho(t) = \sum_{j=-\infty}^{\infty} [\exp(-i\mathbf{L}t)]_{j,0} e^{ij\omega t}\rho(0). \qquad [26]$$

We detect the total x magnetization, $\mathbf{I}_x$, and in Liouville space, this detection is represented by the dot product of $\mathbf{I}_x$ with the density matrix (which is a vector in Liouville space). The detected signal in the time domain is given by

$$\text{signal} = \sum_{j=-\infty}^{\infty} \mathbf{I}_x \cdot [\exp(-i\mathbf{L}t)]_{j,0} e^{ij\omega t}\rho(0). \qquad [27]$$

We can also Fourier transform this equation to get the spectrum as a function of frequency, ν, as in

$$\text{spectrum} = \sum_{j=-\infty}^{\infty} \mathbf{I}_x \cdot \left[\frac{1}{i(2\pi\nu\mathbf{1} + j\omega\mathbf{1} - \mathbf{L})}\right]_{j,0} \rho_{eq}. \qquad [28]$$

These two equations give the spectrum of a spinning single crystal, in either the time or the frequency domain. In order to calculate the spectrum of a powder, these expressions must be averaged over all the possible orientations of a single crystal, i.e., over all the Euler angles, α, β, and γ. Explicit averaging over β and γ is always necessary. The average over α, the angle around the rotor axis, can be done analytically, and it further simplifies Eqs. [27] and [28].

POWDER AVERAGING

Averaging over all orientations is simple, but the straightforward method is very inefficient. Since this process is so important in magnetic resonance, several good algorithms (*49–53*) have been developed. These methods are designed to average over the two Euler angles β and γ. Averaging over α, the angle around the rotor axis, is quite simple, since it is

equivalent to a phase offset in the sample spinning. This average also brings an important simplification (*54*).

To show how to average around the rotor axis, we make the α dependence explicit. This rotation is simply a phase effect, so that equation [13] becomes

$$\mathbf{L}(t) = \sum_{j=-2}^{2} \mathbf{L}^{(j)} e^{ij\omega t} e^{ij\alpha}. \quad [29]$$

When we carry this through the derivation, each of the $\mathbf{L}$ terms in Eq. [23] is modified by a phase factor as in

$$\mathbf{L}^{(j)} \rightarrow \mathbf{L}^{(j)} e^{ij\alpha}. \quad [30]$$

This is a unitary transformation of the full $\mathbf{L}$ matrix, and it is described by a diagonal matrix, $\mathbf{W}$. Because it is unitary, it propagates through any function of $\mathbf{L}$, f($\mathbf{L}$), as in

$$f(\mathbf{W}^{-1}\mathbf{L}\mathbf{W}) = \mathbf{W}^{-1} f(\mathbf{L}) \mathbf{W}. \quad [31]$$

Therefore, the (j, 0) blocks of the matrices in Eq. [27] or [28] are multiplied by $e^{ij\alpha}$ when the sample is rotated through an angle α about the rotor axis.

The powder average over the angle α just averages the signal or the spectrum over all values of the angle. This means that in Eqs. [27] and [28], all the terms with $j \neq 0$ will average to zero. The equations for the time-domain signal, or the frequency-domain spectrum for a powder sample, then become particularly simple. Equation [27] becomes Eq. [32], and Eq. [28] becomes Eq. [33]:

$$\text{signal} = \mathbf{I}_x \cdot [\exp(-i\mathbf{L}t)]_{0,0} \rho(0) \quad [32]$$

$$\text{spectrum} = \left[\frac{1}{i(2\pi\nu\mathbf{1} + j\omega\mathbf{1} - \mathbf{L})} \right]_{0,0} \rho_{eq}. \quad [33]$$

These are very concise and neat formulae for the observables in an MAS experiment. The whole matrix, $\mathbf{L}$, must still be constructed, truncated to the appropriate number of Floquet blocks, and either its exponential or its inverse must be calculated. In practice, however, the full matrix $\mathbf{L}$ does not have to be calculated and stored as a whole, so the programming considerations are eased. Each Floquet block has the dimension of the size of the density matrix, since it is a matrix applied to the density matrix. However, due to the powder averaging, only the central ($j = 0$) block of the inverse (averaged over the other angles, β and γ) is needed to calculate the spectrum.

SPECTRUM CALCULATION

Equation [33] is what we need to calculate the spectrum. However, using this in a numerically efficient manner requires some thought. Inverting the matrix for each frequency, ν, in the spectrum is clearly a waste of computer time. The standard method, usually attributed to Gordon and McGinnis (*46*), involves a single diagonalization of $\mathbf{L}$. Tracing out the spectrum as a function of ν is then quite efficient. Using standard Householder methods, the computational effort to diagonalize a matrix scales as the cube of the size of the matrix. For the number of Floquet blocks needed in an MAS spectrum, this scaling law becomes prohibitive very quickly.

As we noted before, the matrix to be diagonalized has a pentadiagonal structure, and so is inherently sparse. Furthermore, even though diagonalization is computationally intensive, reduction of the matrix to a tridiagonal form can be done relatively quickly. The spectrum can then be calculated from a tridiagonal version of $\mathbf{L}$, using an LU method to solve the system of linear equations associated with Eq. [33]. The Lanczos algorithm (*19*) provides an efficient way of calculating the tridiagonal form of a large, sparse matrix.

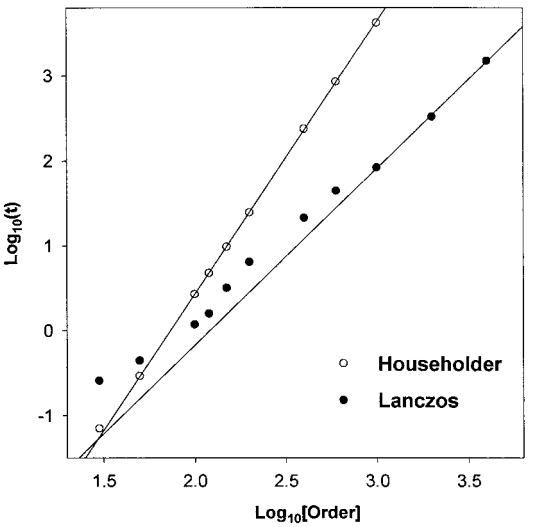

FIG. 1. A comparison between Lanczos and Householder calculations of spinning sideband spectra, showing the scaling of the CPU time with respect to the matrix order. The $\log_{10}$(CPU) is plotted as a function of $\log_{10}$(Order). The slope corresponding to the Householder data (open circles) was 3.2 while that of the Lanczos data (filled circles) was 2.1.

SCALING OF THE CALCULATION

The scaling of Lanczos was compared to Householder by increasing the Floquet dimension, N_F, of a sample system. The spectral range was kept constant; consequently the rotor frequency was inverse proportionately decreased. The logarithm of the CPU time was plotted (Fig. 1) as a function of the logarithm of the matrix order, O, which in the case was $2N_F$. For Householder implementation, the slope of the line was 3.2, which is close to the asymptotic limit 3. The Lanczos method had a slope of 2.1; however, it had significant overhead due to the spectrum evaluation. As in the previous study with liquids

(*24*), saturation behavior was observed for both increased line broadening or with chemical exchange.

The CP/MAS spectra of DMS and [$^{13}C_2$]DMS were simulated using the EisXSS and LanXSS programs. These were written in FORTRAN77, where EisXSS uses Householder and LanXSS uses Lanczos tridiagonalization. Computations were performed on an SGI Octane Dual R10000 at 250 MHz. Programs were compiled with a MIPS 7.21 FORTRAN compiler, with 64-bit word size, running in an Irix 6.5.2 environment.

All simulated spectra contained 4096 points, with an 8000-Hz spectral width. Powder averages, using an approach similar to that of Alderman *et al.* (*53*), were done over 952 points, assuming no symmetry. The sphere was divided into quadrants where one polar angle θ ranged between 0 and 180° and the remaining polar angle ϕ varied from 0 to 90°. The quadrant was divided into $2n$ equally spaced bands parallel to the equator. Each band is divided into curvilinear squares such that squares from different bands subtend approximately the same solid angle. The same pattern is repeated in reverse order for the bottom half of the quadrant. The actual angles used correspond to the center of these squares. The weight for each orientation is equal to the solid angle subtended by the associated square. The linewidths were set to 13 and 75 Hz for DMS and [$^{13}C_2$]DMS, respectively. Rotor speeds ranged from 540 to 580 Hz for the natural abundance sample, and from 320 to 400 Hz for the labeled material. The number of Floquet blocks was 40 for all simulations.

The DMS spectra were simulated as a one-spin two-site mutual exchange, and the [$^{13}C_2$]DMS spectra were simulated as a two-site two-spin nonmutual exchange. Both calculations required matrices of the same size. The $^{12}C,^{13}C$ isotopomer is a one-spin two-site nonmutual exchange problem, whereas the $^{13}C,^{13}C$ case is a two-spin mutual problem. Spectra were simulated (Figs. 3 and 5) for a variety of parameters and compared visually with the experimental spectra (Figs. 2 and 4). Final values were as follows. The principal components of the chemical shift tensor were set at 18.6, 18.6, and −37.3 ppm for both sites; their Euler angles were (0, 0, 0) and (0, 108°, 0). The carbon–carbon internuclear distance of 29 nm, compared to 28 nm in a crystal structure (*55*), gave a slightly better fit. Exchange rates were 50, 800, 1700, and 5500 s^{-1} for temperatures of 295, 333, 343, and 348 K, respectively. Experimental and simulated spectra were compared visually. The EisXSS calculations took 7 min while the LanXSS calculations took 20 min.

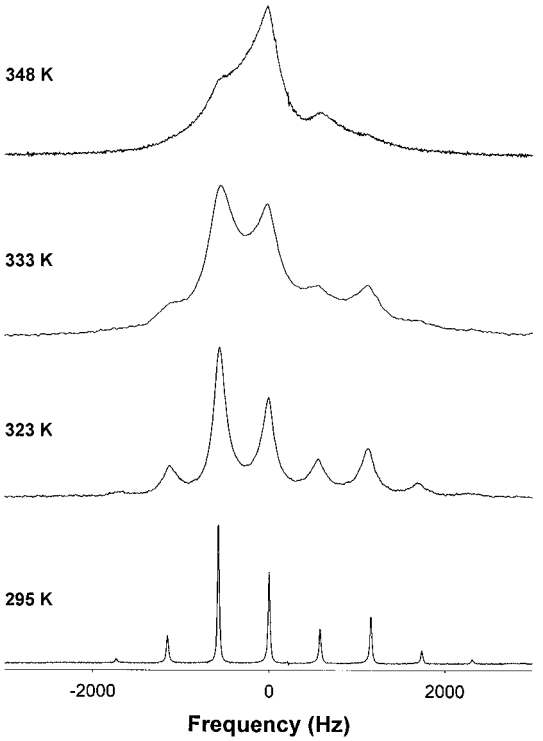

FIG. 2. ^{13}C CP/MAS spectra of unlabeled dimethyl sulfone for a series of temperatures from 295 to 348 K. The spectra were taken at 50 MHz, with a rotor frequency of between 540 and 580 Hz controlled to within 2 to 5 Hz.

CONCLUSIONS

Floquet theory provides an excellent general way of describing the effect of dynamics on an MAS NMR spectrum. The small time-dependent problem is expanded in a Fourier-like series to become a much larger, time-independent problem. This time-independent problem can then be solved using well-established methods from high-resolution NMR system. The numerical disadvantages of increasing the size of the system are substantially avoided by exploiting the inherent sparsity of the Floquet matrices. The Lanczos method for tridiagonalizing a matrix (as opposed to the standard Householder technique) shows much better scaling (between linear and quadratic) as the size of the matrix increases.

The method was tested on CP/MAS spectra of doubly ^{13}C-labeled dimethyl sulfone. In this case, there were both CSA and dipolar interactions, as well as the exchange between the sites. Experimental spectra showed approximately 10 spinning sidebands. These spectra were simulated using both Lanczos and Householder methods. The Lanczos calculation took approximately 20 min on a modern UNIX workstation, and the Householder calculation took about 7 min.

These results establish that the method will work on more complex systems: quadrupolar nuclei, more spins, more interactions. The scaling of the Lanczos methods ensures that the calculations will remain feasible for these important larger systems.

EXPERIMENTAL

Unlabeled dimethyl sulfone was purchased from Aldrich Chemicals and used without further purification. The known (*56*), doubly ^{13}C-labeled dimethyl sulfone (**1**) was prepared from [^{13}C]iodomethane by reaction with sodium sulfide according to the procedure of Tarbell and Weaver (*57*). The resulting presumed dimethyl sulfide was distilled and oxidized

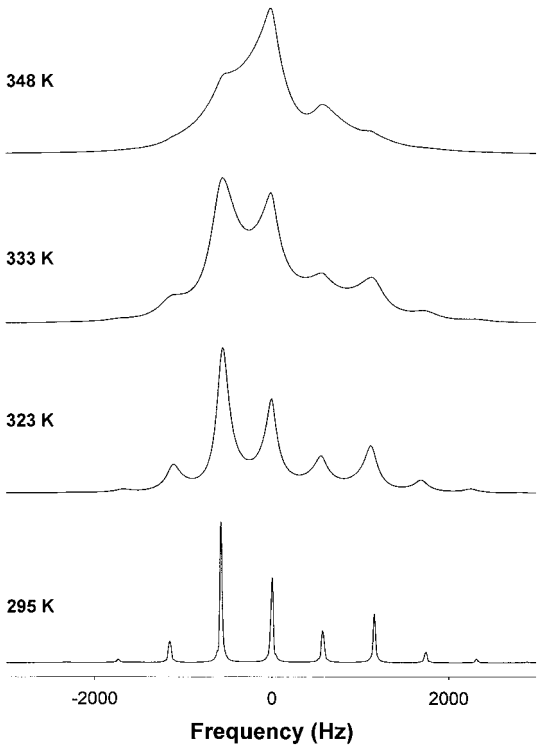

FIG. 3. Simulations of the ^{13}C CP/MAS spectra of unlabeled dimethyl sulfone for a series of temperatures from 295 to 348 K, using EisXSS. Spectral parameters are given in the text.

without further purification using potassium permanganate following the procedure used by Malewski and Mitzinger (*58*) for preparation of [$^{2}H_6$]dimethyl sulfone.

Preparation of [$^{13}C_2$]Dimethyl Sulfone

A mixture of [^{13}C]iodomethane (5 g, 35 mmol) and sodium sulfide nonahydrate (4.6 g, 19 mmol) was heated at reflux with stirring for 4 h, with an attached cold-finger condenser containing an ice-water mixture. The mixture was cooled and distilled through a short path into a fresh flask which was cooled in ice, and to which the cold-finger condenser was attached. The cooled distillate was treated with potassium permanganate (11.5 g) and water (25 mL). After the initial exothermic reaction had subsided, the mixture was heated to reflux in an oil bath (90°C bath temperature) for 5 h while cooling of the cold-finger trap was maintained. The mixture was cooled and stirred at room temperature overnight. The water was removed by distillation, and the solid residue was dried briefly *in vacuo.* The product was sublimed from this black material giving white needles (50 mg, 500 μmol, 3%), mp 106–107°C, 107–108°C for authentic, unlabeled sample (Aldrich); ^{1}H NMR ($CDCl_3$, 200 MHz) δ 2.96 (d, $^{1}J_{^{13}C-H}$ 138 Hz with sidebands due to the magnetic inequivalence of the two carbons); ^{13}C NMR ($CDCl_3$, 50 MHz) δ 42.67 (enriched singlet). A detailed analysis of the proton spectrum (Fig. 2) as an $AA'X_3X_3'$ spin system revealed $^{1}J_{^{13}C-H} = +137.6$ Hz, $^{3}J_{^{13}C-H} = +0.8$ Hz, $^{2}J_{^{13}C-^{13}C} = \pm 9.5$ Hz, and $^{4}J_{H-H} = +0.9$ Hz.

The CP/MAS spectra were acquired on a Bruker DSX-200 spectrometer equipped with a wide-bore magnet of 4.7 T, leading to a proton frequency of 200 MHz and a ^{13}C frequency of 50 MHz. The probe used was a standard Bruker 4-mm double-tuned MAS probe. This probe requires the sample to be packed in a zirconia cylinder of 4 mm diameter and 18 mm length. The sample container is closed by a cap with turbine-like incisions at the outer rim. For magic-angle spinning, the sample is cushioned on a gas stream (bearing) to reduce friction, while a second gas stream blown at an angle over the incisions in the cap drives the rotation. This system had been designed for fast spinning (2 to 16 kHz) and in the standard setup, it was impossible to obtain stable low spinning rates (180 to 800 Hz). Boron nitrate caps which are recommended for variable-temperature studies were used and the turbines were shaved off with a razor blade such that a fairly smooth cone was left. This reduced the driving force sufficiently and the sample could be spun between 180 and 2 kHz.

Temperature control was achieved with a Bruker BVT-3000 unit. This unit regulates the current through a heater in the bearing gas using a copper/constantan thermal coupler as a temperature sensor. The sensor is located close to the sample, also in the bearing gas stream.

The proton 90° pulse length was 5.5 ms, the contact time was 2 ms, and the repetition time was 4 s. The number of

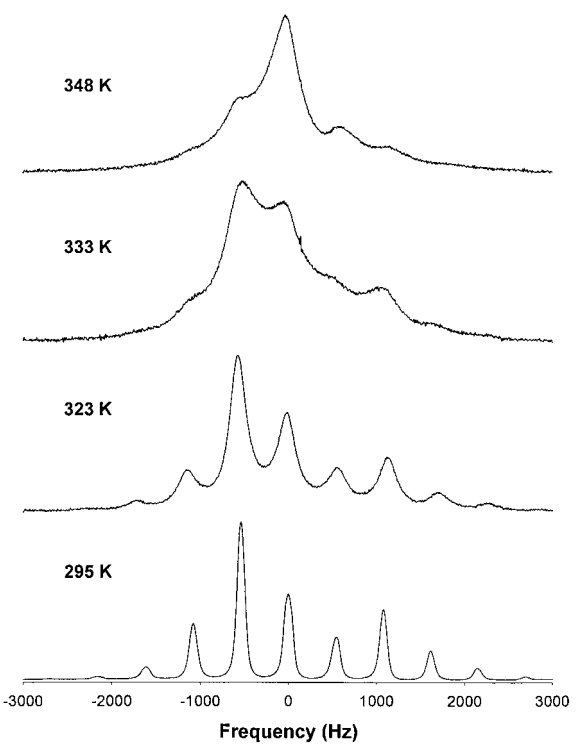

FIG. 4. ^{13}C CP/MAS spectra of doubly ^{13}C-labeled dimethyl sulfone for a series of temperatures from 295 to 348 K. The spectra were taken at 50 MHz, with a rotor frequency of between 320 and 400 Hz controlled to within 2 to 5 Hz.

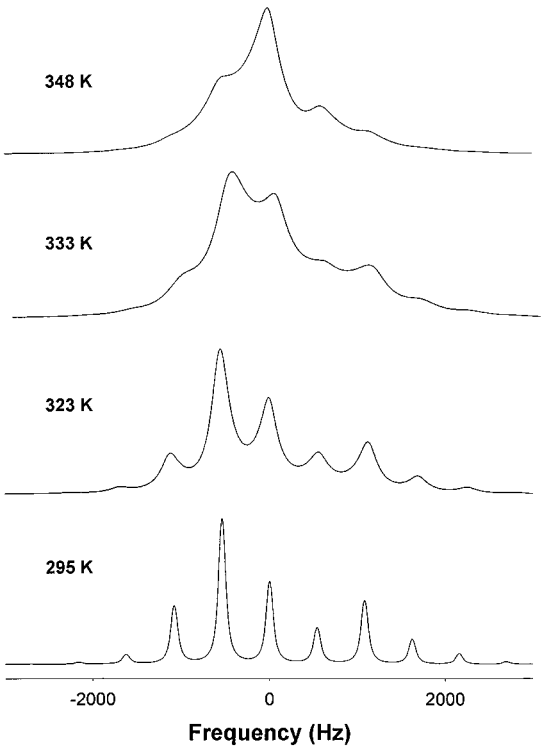

FIG. 5. Simulations of the ^{13}C CP/MAS spectra of doubly ^{13}C-labeled dimethyl sulfone for a series of temperatures from 295 to 348 K, using EisXSS. Spectral parameters are given in the text.

transients varied with each spectrum between 15,000 and 512 in order to obtain similar signal-to-noise ratios (Figs. 3 and 5).

ACKNOWLEDGMENTS

We thank the Natural Sciences and Engineering Research Council of Canada (NSERC) for financial support, Cambridge isotopes for the gift of [^{13}C]methyl iodide, and Valerie Robinson for technical assistance.

REFERENCES

1. J. Schaefer and E. O. Stejskal, Carbon-13 nuclear magnetic resonance of polymers spinning at the magic angle, *J. Am. Chem. Soc.* **98,** 1031–1032 (1976).
2. J. Sandstrom, "Dynamic NMR Spectroscopy," Academic Press, London (1982).
3. L. M. Jackman and F. A. Cotton, "Dynamic Nuclear Magnetic Resonance Spectroscopy," Academic Press, New York (1975).
4. J. R. Lyerla, C. S. Yannoni, and C. A. Fyfe, Chemical applications of variable-temperature CPMAS NMR spectroscopy in solids, *Acc. Chem. Res.* **15,** 208–216 (1982).
5. R. Kubo and K. Tomita, A general theory of magnetic resonance absorption, *J. Phys. Soc. Jpn.* **9,** 888–919 (1954).
6. H. S. Gutowsky and C. H. Holm, Rate processes and nuclear magnetic resonance spectra. II. Hindered internal rotation of amides, *J. Chem. Phys.* **25,** 1228–1234 (1956).
7. D. B. Zax, G. Goelman, D. Abramovich, and S. Vega, Floquet formalism and broadband excitation, *Adv. Magn. Reson.* **14,** 219–240 (1990).
8. D. Abramovich, S. Vega, J. Quant, and S. J. Glaser, The Floquet description of TOCSY and E. TACSY experiments, *J. Magn. Reson. A* **115,** 222–229 (1995).
9. S. Vega, E. T. Olejniczak, and R. G. Griffin, Rotor frequency lines in the nuclear magnetic resonance spectra of rotating solids, *J. Chem. Phys.* **80,** 4832–4840 (1984).
10. T. O. Levante, M. Baldus, B. H. Meier, and R. R. Ernst, Formalized quantum mechanical Floquet theory and its application to sample spinning in nuclear magnetic resonance, *Mol. Phys.* **86,** 1195–1212 (1995).
11. D. Gamliel, Z. Luz, and S. Vega, Complex dynamic NMR-spectra in the fast exchange limit, *J. Chem. Phys.* **85,** 2516–2527 (1986).
12. O. Weintraub and S. Vega, Floquet density matrices and effective Hamiltonians in magic-angle-spinning NMR spectroscopy, *J. Magn. Reson. A* **105,** 245–267 (1993).
13. A. Schmidt and S. Vega, The Floquet theory of magnetic resonance spectroscopy of single spins and dipolar coupled spin-pairs in rotating solids, *J. Chem. Phys.* **96,** 2655–2680 (1992).
14. T. Nakai and C. A. McDowell, Application of Floquet theory to the nuclear magnetic resonance spectra of homonuclear two-spin systems in rotating solids, *J. Chem. Phys.* **96,** 3452–3466 (1991).
15. T. Nakai and C. A. McDowell, Calculation of rotational resonance NMR spectra using Floquet theory combined with perturbation treatment, *Mol. Phys.* **88,** 1263–1275 (1996).
16. S. Ding and C. A. McDowell, The equivalence between Floquet formalism and the multi-step approach in computing the evolution operator of a periodical time dependent Hamiltonian, *Chem. Phys. Lett.* **288,** 230–234 (1998).
17. D. B. Zax, Field-dependent isotropic shifts and limitations to linewidths in solid state nuclear magnetic resonance: A Floquet treatment, *J. Chem. Phys.* **105,** 6616–6625 (1996).
18. A. Schmidt and S. Vega, NMR line-shape analysis for 2-site exchange in rotating solids, *J. Chem. Phys.* **87,** 6895–6907 (1987).
19. G. H. Golub and C. F. van Loan, "Matrix Computations," 3rd ed., Johns Hopkins Univ. Press, Baltimore (1996).
20. G. Moro and J. H. Freed, Calculation of esr spectra and related Fokker–Planck forms by the use of the Lanczos algorithm, *J. Chem. Phys.* **74,** 3757–3773 (1981).
21. K. V. Vasavada, D. J. Schneider, and J. H. Freed, Calculation of ESR spectra and related Fokker Planck forms by the use of the Lanczos algorithm. II. Criteria for truncation of basis sets and recursive steps utilizing conjugate gradients, *J. Chem. Phys.* **86,** 647–661 (1987).
22. G. Moro and J. H. Freed, Classical time correlation functions and the Lanczos algorithm, *J. Chem. Phys.* **75,** 3157–3159 (1981).
23. G. Moro and J. H. Freed, Efficient computation of magnetic resonance spectra and related functions from stochastic Liouville equations, *J. Phys. Chem.* **84,** 2837–2840 (1980).
24. R. S. Dumont, P. Hazendonk, and A. D. Bain, Dual Lanczos simulation of dynamic NMR spectra for systems with many spins or exchange sites, *J. Chem. Phys.,* in press.
25. W. A. Wassam, Jr., Dual Lanczos vector space. I. A formal and numerical framework for the theoretical investigation of relaxation processes, *J. Chem. Phys.* **82,** 3371–3385 (1985).
26. W. A. Wassam, Jr., Dual Lanczos vector space. II. Lanczos transformations and contracted descriptions of relaxation processes, *J. Chem. Phys.* **82,** 3386–3399 (1985).
27. J. H. Wilkinson, "The Algebraic Eigenvalue Problem," Clarendon Press, Oxford (1965).

28. J. H. Shirley, Solutions of the Schrödinger equation with a Hamiltonian periodic in time, *Phys. Rev. B* **138,** 979–987 (1965).
29. Y. Zur and S. Vega, Two-photon NMR on spins with $I = 1$ in solids, *J. Chem. Phys.* **79,** 548–558 (1983).
30. Y. Zur, M. H. Levitt, and S. Vega, Multiphoton NMR spectroscopy on a spin system with $I = \frac{1}{2}$, *J. Chem. Phys.* **78,** 5293–5310 (1983).
31. E. M. Krauss and S. Vega, Four-field excitation of multiphoton NMR resonances in spin $I = \frac{1}{2}$, *Phys. Rev. A* **34,** 333–350 (1986).
32. D. B. Zax and S. Vega, Broadband excitation pulses of arbitrary flip angle, *Phys. Rev. Lett.* **62,** 1840–1843 (1988).
33. G. Goelman, S. Vega, and D. B. Zax, Design of broadband propagators in two-level systems, *Phys. Rev. A* **39,** 5725–5743 (1989).
34. J. Herzfeld and A. E. Berger, Sideband intensities in NMR spectra of samples spinning at the magic angle, *J. Chem. Phys.* **73,** 6021–6030 (1980).
35. M. M. Maricq and J. S. Waugh, NMR in rotating solids, *J. Chem. Phys.* **70,** 3300–3316 (1978).
36. M. M. Maricq, Application of average Hamiltonian theory to the NMR of solids, *Phys. Rev. B* **25,** 6622–6632 (1982).
37. A. Kubo and C. A. McDowell, One- and two dimensional ^{31}P cross-polarization magic-angle-spinning nuclear magnetic resonance studies on two-spin systems with homonuclear dipolar coupling and *J* coupling, *J. Chem. Phys.* **92,** 7156–7170 (1990).
38. A. Schmidt and S. Vega, The transition amplitudes of centerband and sidebands in NMR spectra of rotating solids, *Isr. J. Chem.* **32,** 215–230 (1992).
39. A. Schmidt, R. G. Griffin, D. P. Raleigh, J. E. Roberts, S. O. Smith, and S. Vega, Chemical-exchange effects in the NMR-spectra of rotating solids, *J. Chem. Phys.* **85,** 4248–4253 (1986).
40. Z. Luz, R. Poupko, and S. Alexander, Theory of dynamic magic-angle-spinning nuclear magnetic resonance and its application to ^{13}C in solid bullvalene, *J. Chem. Phys.* **99,** 7544–7553 (1993).
41. A. D. Bain, The superspin formalism for pulse NMR, *Prog. NMR Spectrosc.* **20,** 295–315 (1988).
42. G. Binsch, A unified theory of exchange effects on nuclear magnetic resonance lineshapes, *J. Am. Chem. Soc.* **91,** 1304–1309 (1969).
43. A. D. Bain and G. J. Duns, A unified approach to dynamic nmr based on a physical interpretation of the transition probability, *Can. J. Chem.* **74,** 819–824 (1996).
44. U. Fano, *in* "Lectures on the Many Body Problem" (E. R. Caianiello, Ed.), Vol. 2, pp. 217–239, Academic Press, New York (1964).
45. C. N. Banwell and H. Primas, On the analysis of high-resolution nuclear magnetic resonance spectra. I. Methods of calculating NMR spectra, *Mol. Phys.* **6,** 225–256 (1963).
46. R. G. Gordon and R. P. McGinnis, Lineshapes in molecular spectra, *J. Chem. Phys.* **49,** 2455–2456 (1968).
47. R. S. Dumont, A. D. Bain, and S. Jain, Simulation of many-spin system dynamics via sparse matrix methodology, *J. Chem. Phys.* **106,** 5928–5936 (1997).
48. H. Tal-Ezer and R. Kosloff, An accurate and efficient scheme for propagating the time dependent Schrödinger equation, *J. Chem. Phys.* **81,** 3967–3971 (1984).
49. M. Mombourquette and J. A. Weil, Simulation of magnetic resonance powder spectra, *J. Magn. Reson.* **99,** 37–44 (1992).
50. D. Wang and G. R. Hanson, A new method for simulating randomly oriented powder spectra in magnetic resonance: The Sydney Opera House (SOPHE) method, *J. Magn. Reson. A* **117,** 1–8 (1995).
51. M. Bak and N. C. Neilsen, REPULSION, a novel approach to efficient powder averaging in solid state NMR, *J. Magn. Reson.* **125,** 132–139 (1997).
52. S. J. Varner, R. L. Vold, and G. L. Hoatson, An efficient method for calculating powder patterns, *J. Magn. Reson. A* **123,** 72–80 (1997).
53. D. W. Alderman, M. S. Solum, and D. M. Grant, Methods for analyzing spectroscopic lineshapes. NMR solid state powder patterns, *J. Chem. Phys.* **84,** 3717–3725 (1986).
54. T. Charpentier, C. Fermon, and J. Virlet, Efficient time propagation for MAS NMR simulation. Application to quadrupolar nuclei, *J. Magn. Reson.* **132,** 181–190 (1998).
55. D. A. Langs, J. V. Silverton, and W. M. Bright, Chemical analysis by X-ray crystallography—Structure of dimethyl sulfone, *J. Chem. Soc., Chem. Commun.,* 1653–1654 (1970).
56. S. Saito and F. Makino, The microwave spectrum of dimethylsulfone, *Bull. Chem. Soc. Jpn.* **45,** 92–94 (1972).
57. D. S. Tarbell and C. Weaver, The condensation of sulfoxides with *p*-toluenesulfonamide and substituted acetamides, *J. Am. Chem. Soc.* **63,** 2939–2942 (1941).
58. G. Malewski and L. Mitzinger, Preparation of dimethylsulfone-d_6, *Monatsber. Dtsch. Akad. Wiss. Berlin* **10,** 74–75 (1968).